https://doi.org/10.5194/hess-2020-315
Preprint. Discussion started: 7 August 2020

Hydrology and Earth System Sciences
Discussions

Technical Note: Partial wavelet coherency for improved understanding of scale-specific and localized bivariate relationships in geosciences

Wei Hu[1] and Bing Si[2]

[1]*The New Zealand Institute for Plant and Food Research Limited, Private Bag 4704, Christchurch 8140, New Zealand*

[2]*University of Saskatchewan, Department of Soil Science, Saskatoon, SK S7N 5A8, Canada*

Correspondence to: Wei Hu (wei.hu@plantandfood.co.nz)

Abstract

Bivariate wavelet coherency is widely used to untangle the scale-specific and localized bivariate relationships in geosciences. However, it is well-known that bivariate relationships can be misleading when both variables are correlated to other variables. Partial wavelet coherency (PWC) has been proposed, but is limited to one excluding variable and presents no phase information. We aim to develop a new PWC method that can deal with multiple excluding variables and presents phase information for the PWC. Tests with both stationary and non-stationary artificial datasets verified the known scale- and localized bivariate relationships after eliminating the effects of other variables. Compared with the previous PWC method, the new method has the advantages of capturing phase information, dealing with multiple excluding variables, and producing more accurate results. The new method was also applied to two field measured datasets. Results showed that the coherency

https://doi.org/10.5194/hess-2020-315
Preprint. Discussion started: 7 August 2020


Hydrology and Earth System Sciences
Discussions

between response and predictor variables was usually less affected by excluding variables when predictor variables had higher correlation with the response variable. Application of the new method also confirmed the best predictor variables for explaining temporal variations in free water evaporation at Changwu site in China and spatial variations in soil water content in a hummocky landscape in Saskatchewan Canada. We suggest the PWC method to be used in combination with previous wavelet methods to untangle the scale-specific and localized multivariate relationships in geosciences. The PWC calculations were coded with Matlab and are available in the supplement.

1. Introduction

Geoscience data, such as spatial distribution of soil moisture in undulating terrains and temporal series of climatic variables, usually consist of a variety of transient processes with different frequencies (scales) that may be localized in time or space (Graf et al., 2014; Si, 2008; Torrence and Compo, 1998). Wavelet methods are widely used to detect scale-specific and localized features of geoscience data irrespective of whether they are stationary or non-stationary. Among which, bivariate wavelet coherency (BWC) is widely accepted as a tool for detecting scale-specific and localized bivariate relationships in a range of areas in geoscience (Biswas and Si, 2011a; Das and Mohanty, 2008; Lakshmi et al., 2004; Polansky et al., 2010; Si and Zeleke, 2005). Recently, Hu and Si (2016) have extended the BWC to multiple wavelet coherence (MWC) that can be used to untangle multivariate (≥3 variables) relationships in multiple scale-location domains. This method has been successfully used in hydrology (Gu et al., 2020; Hu et al., 2017; Mares et al., 2020; Nalley et al., 2019; Su et

https://doi.org/10.5194/hess-2020-315
Preprint. Discussion started: 7 August 2020


Hydrology and Earth System Sciences
Discussions

al., 2019) and other areas such as soil science (Centeno et al., 2020), environmental science (Zhao et al., 2018), climate (Song et al., 2020), and economics (Sen et al., 2019).

The MWC application has shown that an increased number of predictor variables does not necessarily explain more variation in the response variable, partly because predictor variables are usually cross-correlated (Hu and Si, 2016). For the same reason, bivariate relationships can be misleading if the predictor variable is correlated with other variables that control the response variable. Partial correlation analysis is one such method to deal with this issue (Kenney and Keeping, 1939), but the extension of partial correlation to the multiple scale-location domain is limited. In order to better understand the bivariate relationships at multiple scales and locations, the BWC needs to be extended to partial wavelet coherency (PWC) by eliminating the effects of other variables.

The BWC was extended to PWC by Mihanović et al. (2009). Their method has been widely employed in the areas of marine science (Ng and Chan, 2012a, b), climate (Rathinasamy et al., 2017; Tan et al., 2016), greenhouse gas emissions (Jia et al., 2018; Li et al., 2018; Mutascu and Sokic, 2020), and economics (Aloui et al., 2018; Altarturi et al., 2018; Wu et al., 2020), among others. However, Mihanović et al. (2009) considered one excluding variable only and did not include the phase angle difference between response and predictor variables.

As an extension of previous studies (Hu and Si, 2016; Mihanović et al., 2009), this paper aims to develop a PWC method that considers more than one excluding variable and phase information. The new method is developed in analogy with the partial coherency in the

https://doi.org/10.5194/hess-2020-315
Preprint. Discussion started: 7 August 2020


Hydrology and Earth System Sciences
Discussions

multiple spectral case (Koopmans, 1995). It is first tested with artificial datasets following Yan and Gao (2007) and Hu and Si (2016) to demonstrate its capability of capturing the known relationships of the artificial data. Next, the new method is compared with the Mihanović et al. (2009) method. Then it is applied to two real (i.e., field measured) datasets in geosciences including temporal series of free water evaporation at the Changwu site in China (Hu and Si, 2016) and spatial series of soil water content from a transect in the hummocky landscape in Saskatchewan, Canada (Biswas and Si, 2011a; Hu et al., 2017). These two datasets are chosen because the MWC results previously presented (Hu and Si, 2016; Hu et al., 2017) can be used to assess the new method.

2. Theory

Similar to BWC and MWC, PWC is calculated from auto- and cross-wavelet power spectra, for the response variable y, predictor variable x, and excluding variables Z ($Z = \{Z_1, Z_2, \cdots, Z_q\}$). In analogy with the partial coherency in the multivariate spectral case (Koopmans, 1995), the complex PWC between y and x after excluding variables Z at scale s and location τ, $\gamma_{y,x\cdot Z}$, can be written as:

$$\gamma_{y,x\cdot Z}(s,\tau) = \frac{\left(1 - R^2_{y,x\cdot Z}(s,\tau)\right)\gamma_{y,x}(s,\tau)}{\left(\left(1 - R^2_{y,Z}(s,\tau)\right)\left(1 - R^2_{x,Z}(s,\tau)\right)\right)^{1/2}} \quad (1)$$

where $R^2_{y,x\cdot Z}(s,\tau)$, $R^2_{y,Z}(s,\tau)$, and $R^2_{x,Z}(s,\tau)$ can be calculated by following Hu and Si (2016) as

https://doi.org/10.5194/hess-2020-315
Preprint. Discussion started: 7 August 2020

Hydrology and Earth System Sciences
Discussions

$$R^2_{y,x\cdot Z}(s,\tau) = \frac{\overleftrightarrow{W}^{y,Z}(s,\tau)\,\overleftrightarrow{W}^{Z,Z}(s,\tau)^{-1}\,\overline{\overleftrightarrow{W}^{x,Z}(s,\tau)}}{\overleftrightarrow{W}^{y,x}(s,\tau)} \quad (2)$$

$$R^2_{y,Z}(s,\tau) = \frac{\overleftrightarrow{W}^{y,Z}(s,\tau)\,\overleftrightarrow{W}^{Z,Z}(s,\tau)^{-1}\,\overline{\overleftrightarrow{W}^{y,Z}(s,\tau)}}{\overleftrightarrow{W}^{y,y}(s,\tau)} \quad (3)$$

$$R^2_{x,Z}(s,\tau) = \frac{\overleftrightarrow{W}^{x,Z}(s,\tau)\,\overleftrightarrow{W}^{Z,Z}(s,\tau)^{-1}\,\overline{\overleftrightarrow{W}^{x,Z}(s,\tau)}}{\overleftrightarrow{W}^{x,x}(s,\tau)} \quad (4)$$

$\gamma_{y,x}(s,\tau)$ is the complex wavelet coherence between y and x, which can be written as

$$\gamma_{y,x}(s,\tau) = \frac{\overleftrightarrow{W}^{y,x}(s,\tau)}{\left(\overleftrightarrow{W}^{y,y}(s,\tau)\overleftrightarrow{W}^{x,x}(s,\tau)\right)^{1/2}} \quad (5)$$

where $\overleftrightarrow{(\cdot)}$ is the smoothing operator, $\overline{(\cdot)}$ is the complex conjugate operator, $(\cdot)^{-1}$ indicates the inverse of the matrix, and

$$\overleftrightarrow{W}^{y,Z}(s,\tau) = \left[\overleftrightarrow{W}^{y,Z_1}(s,\tau)\,\overleftrightarrow{W}^{y,Z_2}(s,\tau)\cdots\overleftrightarrow{W}^{y,Z_q}(s,\tau)\right] \quad (6)$$

$$\overleftrightarrow{W}^{x,Z}(s,\tau) = \left[\overleftrightarrow{W}^{x,Z_1}(s,\tau)\,\overleftrightarrow{W}^{x,Z_2}(s,\tau)\cdots\overleftrightarrow{W}^{x,Z_q}(s,\tau)\right] \quad (7)$$

$$\overleftrightarrow{W}^{Z,Z}(s,\tau) = \begin{bmatrix} \overleftrightarrow{W}^{Z_1,Z_1}(s,\tau) & \cdots & \overleftrightarrow{W}^{Z_1,Z_q}(s,\tau) \\ \vdots & \ddots & \vdots \\ \overleftrightarrow{W}^{Z_q,Z_1}(s,\tau) & \cdots & \overleftrightarrow{W}^{Z_q,Z_q}(s,\tau) \end{bmatrix} \quad (8)$$

where $\overleftrightarrow{W}^{A,B}(s,\tau)$ is the smoothed auto-wavelet power spectra (when A=B) or cross-wavelet power spectra (when $A\neq B$) at scale s and location τ, respectively. Please refer to previous publications for detailed calculation of smoothed auto- and cross-wavelet power spectra (Grinsted et al., 2004; Hu and Si, 2016).

https://doi.org/10.5194/hess-2020-315
Preprint. Discussion started: 7 August 2020


Hydrology and Earth System Sciences
Discussions

94 The squared PWC (hereinafter referred to as PWC) at scale s and location τ, $\rho^2_{y,x\cdot Z}$,
95 can be written as

96 $$\rho^2_{y,x\cdot Z} = \frac{\left|1-R^2_{y,x\cdot Z}(s,\tau)\right|^2 R^2_{y,x}(s,\tau)}{\left(1-R^2_{y,Z}(s,\tau)\right)\left(1-R^2_{x,Z}(s,\tau)\right)} \quad (9)$$

97 where

98 $$R^2_{y,x}(s,\tau) = \frac{\overleftrightarrow{W}^{y,x}(s,\tau)\overleftrightarrow{W^{y,x}(s,\tau)}}{\overleftrightarrow{W}^{y,y}(s,\tau)\overleftrightarrow{W}^{x,x}(s,\tau)} \quad (10)$$

99 The phase angle between y and x after excluding effect of Z is

100 $$\vartheta_{y,x\cdot Z}(s,\tau) = \varphi_{y,x\cdot Z}(s,\tau) + \vartheta_{y,x}(s,\tau) \quad (11)$$

101 where

102 $$\varphi_{y,x\cdot Z}(s,\tau) = \arg\left(1 - R^2_{y,x\cdot Z}(s,\tau)\right) \quad (12)$$

103 and $\vartheta_{y,x}(s,\tau)$ is the wavelet phase between y and x, which can be expressed as

104 $$\vartheta_{y,x}(s,\tau) = \tan^{-1}\left(\mathrm{Im}\left(W^{y,x}(s,\tau)\right)/\mathrm{Re}\left(W^{y,x}(s,\tau)\right)\right) \quad (13)$$

105 where arg denote the argument of the complex number, $W^{y,x}(s,\tau)$ is the cross-wavelet
106 power spectrum between y and x at scale s and location τ; Im and Re denote the
107 imaginary and real part of $W^{y,x}(s,\tau)$, respectively.

108 The Monte Carlo method is used to calculate PWC at 95% confidence level. In brief,
109 calculation of PWC is repeated for a sufficient number of times using data generated by
110 Monte Carlo simulations based on the first-order autocorrelation coefficient. The 95th

https://doi.org/10.5194/hess-2020-315
Preprint. Discussion started: 7 August 2020


Hydrology and Earth System Sciences
Discussions

percentile of PWCs of all simulations at each scale represents the PWC at the 95% confidence level. The average PWC, percent area of significant coherence (PASC) relative to the whole wavelet scale–location domain, and average value of significant PWC (PWC_{sig}) are also calculated for different scale-location domains. The Matlab codes for calculating PWC and significance level are provided in the Supplement (Sect. S1–S3).

The new method is compared with the method of Mihanović et al. (2009) in the case of one excluding variable ($Z = \{Z_1\}$). The Mihanović et al. (2009) method was developed directly from the traditional partial correlation analysis (Kenney and Keeping, 1939), and therefore has a similar equation for calculating PWC, which can be expressed as

$$\rho^2_{y,x\cdot Z1} = \frac{\left|R_{y,x}(s,\tau) - R_{y,Z1}(s,\tau)\, R_{x,Z1}(s,\tau)\right|^2}{\left(1-R^2_{y,Z1}(s,\tau)\right)\left(1-R^2_{x,Z1}(s,\tau)\right)} \qquad (14)$$

In the case of one excluding variable, the numerators between Eqs. (9) and (14) differ, but the denominators remain the same.

3. Data and analysis

3.1 Artificial data for method test

The PWC is first tested using the cosine-like artificial dataset produced following Yan and Gao (2007). The cosine-like artificial datasets are suitable for testing the new method because they mimic many spatial or temporal series in geoscience such as climatic variables, hydrologic fluxes, seismic signals, El Niño-Southern Oscillation, land surface topography, ocean waves, and soil moisture. The procedures to test the PWC is largely based on Hu and

https://doi.org/10.5194/hess-2020-315
Preprint. Discussion started: 7 August 2020


Hydrology and Earth System Sciences
Discussions

Si (2016), where the same dataset has been used to test the MWC method. Please refer to Hu and Si (2016) for the detailed description of the artificial dataset. In brief, the response variable (y and z for the stationary and non-stationary case, respectively) is the sum of five cosine waves (y_1 to y_5 and z_1 to z_5 for the stationary and non-stationary case, respectively) at 256 locations (Hu and Si, 2016). For y_1, y_2, y_3, y_4, and y_5, they have consistent dimensionless scales of 4, 8, 16, 32, and 64, respectively, across the series. For z_1, z_2, z_3, z_4, and z_5, the dimensionless scales gradually change with location, with the maximum dimensionless scales of 4, 8, 16, 32, and 64, respectively. The variance of the response variable y and z is 2.5. All other variables (y_1 to y_5 or z_1 to z_5) are orthogonal to each other with equal variance of 0.5. The predictor and excluding variables (Fig. S1 of Sect. S4 in the Supplement) are selected from the five cosine waves (e.g., y_1 to y_5 or z_1 to z_5) or their derivatives. The exact variables and procedures to test the new PWC method are explained later on.

The PWC between response variable y (or z) and predictor variable, i.e., y_2 (or z_2), is first calculated after excluding the effect of one variable. Four types of excluding variable are involved (Fig. S1 of Sect. S4 in the Supplement): (a) original series of y_2 (or z_2) or y_4 (or z_4); (b) second half of the original series of y_2 (or z_2) are replaced by 0 to simulate abrupt changes (i.e., transient and localized feature) of the spatial series. They are referred to as y_2h_0 (*or* z_2h_0); (c) white noises with zero-mean and standard deviations of 0.3 (weak noise), 1 (moderate noise), and 4 (high noise) are added to y_2 (or z_2) as suggested by Hu and Si (2016) to simulate non-perfect cyclic patterns of the excluding variables. They are referred to as y_2wn (*or* z_2wn), y_2mn (*or* z_2mn), and y_2sn (*or* z_2sn), respectively; and (d) a combination

https://doi.org/10.5194/hess-2020-315
Preprint. Discussion started: 7 August 2020


Hydrology and Earth System Sciences
Discussions

of type b and type c. They are referred to as y_2wnh_0 (*or* z_2wnh_0), y_2mnh_0 (*or* z_2mnh_0), and y_2snh_0 (*or* z_2snh_0), respectively. The same data are also analyzed using the Mihanović et al. (2009) method for comparison.

The PWC between response variable y (or z) and predictor variable, i.e., y_2y_4 (sum of y_2 and y_4) for the stationary case or z_2z_4 (sum of z_2 and z_4) for the non-stationary case, is calculated with two excluding variables, which is a combination of y_4 (or z_4) and y_2 (or z_2) or its noised series (y_2wn *or* z_2wn, y_2mn *or* z_2mn, and y_2sn *or* z_2sn). Note that PWC between y (or z) and other predictor variables (e.g., y_4 or z_4) after excluding y_2 or z_2 and their equivalent derivative variables (i.e., noised variables or variables with 0) are also calculated. The related results are not shown because they are analogous to those in case of predictor variable of y_2 (or z_2).

The merit of the artificial data is that we know the exact scale- and localized bivariate relationships after the effect of excluding variables is removed. Theoretically, we expect (a) PWC is 1 at scales corresponding to scale difference of excluding variables from predictor variable, and 0 at other scales. For example, PWC between y and y_2y_4 after excluding the effect of y_4 is expected to be 1 at the scale of 8, which is the difference of y_4 (32) from y_2y_4 (8 and 32), and 0 at other scales (e.g., 32); (b) PWC remains 1 at the second half of series where spatial series is replaced by 0, and 0 at the first half of the original series. For example, PWC between y and y_2 after excluding the effect of y_2h_0 is expected to be 0 and 1 at the first and second half of series, respectively, at the scale of 8; and (c) PWC increases as more noises are included in the excluding variables. For example, PWC between y and y_2 after

https://doi.org/10.5194/hess-2020-315
Preprint. Discussion started: 7 August 2020


Hydrology and Earth System Sciences
Discussions

173 excluding the effect of noised series of y_2 is expected to increase with increasing noises in
174 an order of $y_2sn > y_2mn > y_2wn$ at the scale of 8.

175 **3.2 Real data for application**

176 3.2.1 Free water evaporation

177 The free water evaporation dataset has been used to test the MWC (Hu and Si, 2016). In
178 brief, this dataset includes monthly free water evaporation (E), mean temperature (T),
179 relative humidity (RH), sun hours (SH), and wind speed (WS) between January 1979 and
180 December 2013 at Changwu site in Shaanxi province provided by the China Meteorological
181 Administration. During this period, the average daily temperature was 9.4 °C, the average
182 annual rainfall was 571 mm and annual ET_p was 883 mm. Being located in the transition
183 between semi-arid and subhumid climates, agricultural production at the Changwu site is
184 constrained by water availability. The PWC between E and each meteorological variable is
185 calculated by excluding the effect of each or all of the other meteorological variables.
186 Results of wavelet power spectrum of E and BWC between every two variables are shown
187 in Fig. S2 and Fig. S3 (Sect. S5 in the Supplement), respectively.

188 3.2.2 Soil water content

189 Soil water datasets were obtained from the hummocky landscape of Canadian Prairies
190 (Biswas and Si, 2011b; Hu et al., 2017). The sampling site is characterized by a subhumid
191 continental climate with Dark Brown Chernozem soils. Data were collected from 128
192 locations with equal intervals (4.5 m) along a 576 m long transect. Soil water contents of

https://doi.org/10.5194/hess-2020-315
Preprint. Discussion started: 7 August 2020


Hydrology and Earth System Sciences
Discussions

top layer (0–0.2 m) were measured by a portable Tektronix TDR in spring (May 2, 2008) and summer (August 23, 2008). Other environmental variables measured were clay content, sand content, soil organic carbon content (SOC), bulk density (BD) of 0–0.2 m, depth to $CaCO_3$ layer (vertical distance between surface and the layer of first presence of $CaCO_3$), elevation, slope, aspect (calculated as cos(aspect)), and wetness index. Please refer to previous studies for detailed information on this dataset (Biswas et al., 2012; Biswas and Si, 2011a, b).

The PWC between SWC and each environmental variable is calculated by excluding the effect of another environmental factor. The BWC between SWC and each environmental factor (Fig. S4 and S5 of Sect. S5 in the Supplement), BWC between environmental factors (Fig. S6 of Sect. S5 in the Supplement), and MWC between SWC and environmental factors have been previously analyzed (Biswas and Si, 2011a; Hu et al., 2017).

4. Results and discussion

4.1 PWC with artificial data

4.1.1 PWC with one excluding variable using the new method

Fig. 1a shows PWC between dependent variable y (or z) and predictor variable y_2 (or z_2) by excluding one variable. For the stationary case, there is one horizontal band (red color) representing an in-phase high PWC value at scales around 8 for all locations after eliminating the effect of y_4. Note that the PWC values between y and y_2 after excluding the effect of y_4 are not exactly 1 as would be expected at all scale-location domains, because of

https://doi.org/10.5194/hess-2020-315
Preprint. Discussion started: 7 August 2020

Hydrology and Earth System Sciences
Discussions

the effect of smoothing along scales and locations. However, the PWC values at the center of the significant band, corresponding to the exact scale (8) of the predictor variable y_2, are very close to 1 (0.996), and the mean PWC_{sig} values are very high (i.e., 0.96). The result is similar to the BWC between y and y_2. This is understandable because y_4 is orthogonal to y_2, and excluding the effect of y_4 does not affect the relationship between y and y_2 at all.

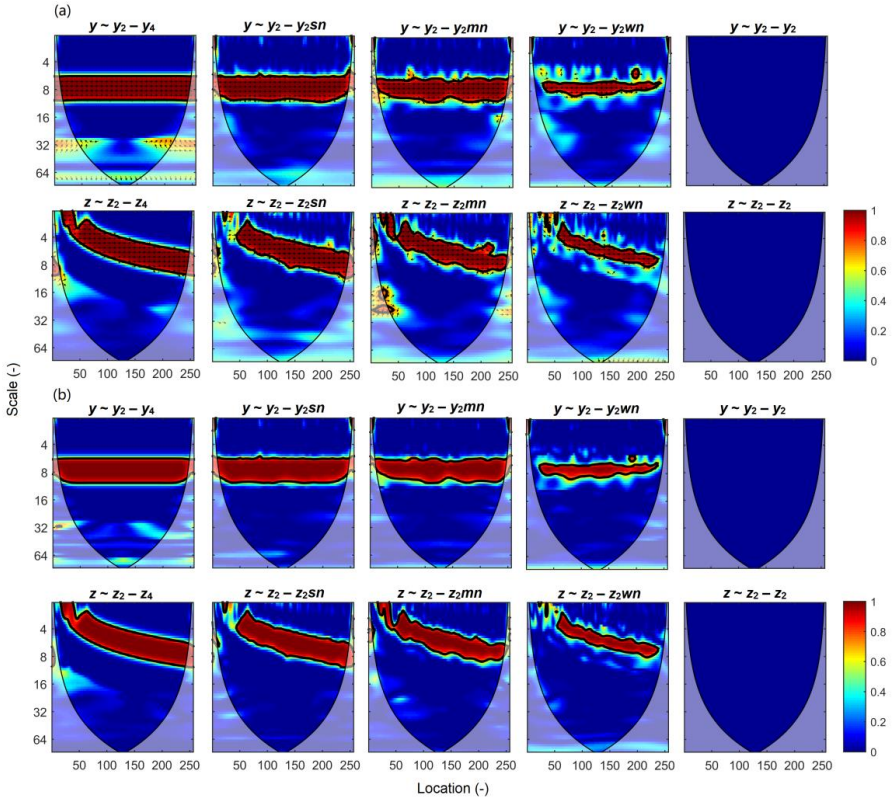

Figure 1.

Partial wavelet coherency (PWC) between response variable y (or z) and predictor variable y_2 (or z_2) after excluding the effect of variables y_4 (or z_4), y_2sn (or z_2sn), y_2mn (or z_2mn), y_2wn (or z_2wn), and y_2 (or z_2) for the stationary (or non-stationary) case using the new

https://doi.org/10.5194/hess-2020-315
Preprint. Discussion started: 7 August 2020


Hydrology and Earth System Sciences
Discussions

method (a) and Mihanović et al. (2009) method (b). Arrows represent the phase angles of the cross-wavelet power spectra between two variables after eliminating the effect of excluding variables. Arrows pointing to the right (left) indicate positive (negative) correlations. Thin and thick solid lines show the cones of influence and the 95% confidence levels, respectively. All variables are explained in Section 3.1 and are shown in Fig. S1 of Sect. S4 in the Supplement.

Similar results were obtained by excluding either y_4 or the strongly noised series of y_2 (y_2sn). Compared with the case of excluding variable of y_4, excluding the effect of y_2sn results in slightly narrower band of significant PWC and slightly reduced mean PWC_{sig} (0.94 versus 0.96). When less noise is included in the excluding variables (i.e., y_2mn and y_2wn), the significant PWC band becomes narrower. The PASC values are 86%, 77%, and 32% for excluding y_2sn, y_2mn and y_2wn, respectively, at scales of 6–10. Moreover, the mean PWC_{sig} decreases from 0.94 (y_2sn) to 0.93 (y_2mn) and 0.89 (y_2wn) when progressively more noise is added (Fig. 1a). If we exclude the predictor variable y_2 itself, there are, as we expect, no correlations between y and y_2 (Fig. 1a). For the non-stationary case, similar results are obtained (Fig. 1a). The only difference is that the scales with significant PWC values change with location, as is found for MWC (Hu and Si, 2016).

https://doi.org/10.5194/hess-2020-315
Preprint. Discussion started: 7 August 2020

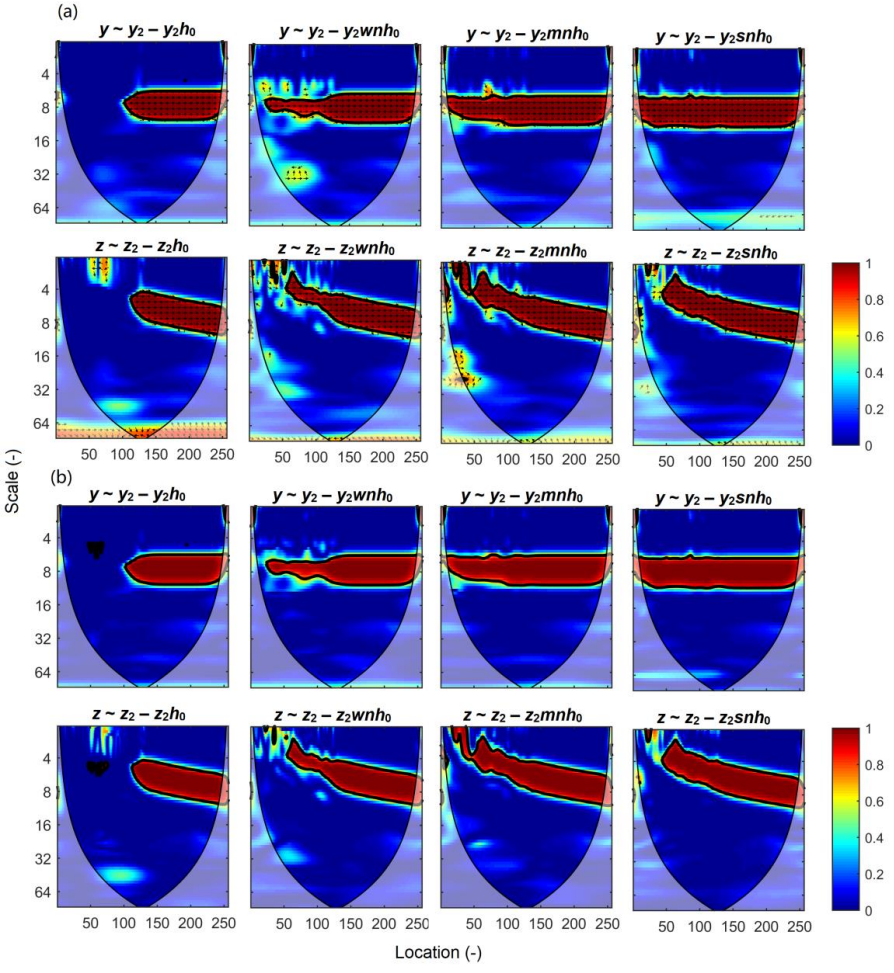

Figure 2.

Partial wavelet coherency (PWC) between response variable y (or z) and predictor variable y_2 (or z_2) after excluding effect of variables y_2h_0 (or z_2h_0), y_2wnh_0 (or z_2wnh_0), y_2mnh_0 (or z_2mnh_0), and y_2snh_0 (or z_2snh_0), for the stationary (or non-stationary) case using the new method (a) and Mihanović et al. (2009) method (b). All variables are explained in Section 3.1 and are shown in Fig. S1 of Sect. S4 in the Supplement.

When second half of the excluding variable series is replaced by 0, the PWC values in that half are close to 1, while those in the first half of data series are 0 at scales

https://doi.org/10.5194/hess-2020-315
Preprint. Discussion started: 7 August 2020


Hydrology and Earth System Sciences
Discussions

corresponding to the predictor variable (Fig. 2a). For the stationary case, after excluding the effect of y_2h_0, the PWC values are close to 1 (0.98) and 0 in the second and first half of the data series, respectively, at the dimensionless scale of 8 (Fig. 2a). Similar results are observed for the non-stationary case (Fig. 2a). This is anticipated because removing series of 0s from a portion of the predictor variable series does not affect their correlations at these locations. If different magnitudes of noises are added to the first half of the excluding variables (y_2 or z_2), the significant PWC band in the first half becomes wider as the magnitude of noises increases, while the significant PWC band in the second half remains almost unchanged. Take the stationary case for example, the PASC values at scales of 6–10 are 40% (y_2wnh_0), 74% (y_2mnh_0), and 86% (y_2snh_0) in the first half, respectively, while those values vary from 86% to 90% in the second half. Meanwhile, the mean PWC_{sig} in the first half at scales of 6–10 increases from 0.91 to 0.94 in both the stationary and non-stationary cases as more noises are added to the excluding variable y_2 or z_2. This indicates that the new PWC method can also capture the abrupt changes in the data series, and has the ability to deal with localized relationships.

4.1.2 PWC with two excluding variables using the new method

When both y_2 and y_4 (or z_2 and z_4) are considered in the predictor variables, there are two bands of wavelet coherence of 1 between y (or z) and y_2y_4 (or z_2z_4), which correspond to the scales of two predictor variables (Hu and Si, 2016). However, after the effect of y_4 (or z_4) is removed, only one band with PWC of around 1 occurs at the scale of the predictor variable y_2 (or z_2) (Fig. 3), which is identical to the PWC between y (or z) and y_2 (or z_2) after

https://doi.org/10.5194/hess-2020-315
Preprint. Discussion started: 7 August 2020

Hydrology and Earth System Sciences
Discussions

excluding the effect of variable y_4 (or z_4) (Fig. 1). After both predictor variables y_2 and y_4 (or z_2 and z_4) are excluded, the PWC between y (or z) and y_2y_4 (or z_2z_4) is 0 at all scale-location domains as we expect. When one of the excluding variables y_2 (or z_2) is added with noises, the relationship between response variable y (or z) and predictor variable y_2y_4 (or z_2z_4) becomes significant at scales of the excluding variable y_2 (or z_2). Similar to the case of one excluding variable (Fig. 1), less noise in the excluding variable of y_2 (or z_2) results in narrower significant PWC band, and reduced mean PWC_{sig} values (from 0.96 (y_2sn) to 0.90 (y_2wn) in the stationary case and from 0.95 (z_2sn) to 0.92 (z_2wn) in the non-stationary case) (Fig. 3).

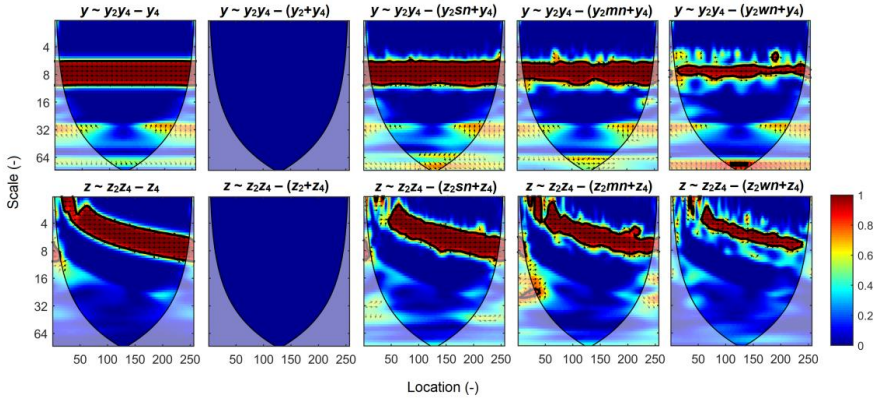

Figure 3.

Partial wavelet coherency (PWC) between response variable y (or z) and predictor variable y_2y_4 (or z_2z_4) after excluding the effect of variables y_4 (or z_4), y_2+y_4 (or z_2+z_4), y_2sn+y_4 (or z_2sn+z_4), y_2mn+y_4 (or z_2mn+z_4), and y_2wn+y_4 (or z_2wn+z_4) for the stationary (or non-stationary) case. All variables are explained in Section 3.1 and are shown in Fig. S1 of Sect. S4 in the Supplement.

https://doi.org/10.5194/hess-2020-315
Preprint. Discussion started: 7 August 2020

4.1.3 Comparison of the new method with the Mihanović et al. (2009) method

In the case of one excluding variable, the corresponding PWC values calculated with the Mihanović et al. (2009) method are shown in Figs 1b and 2b. Except for the phase information, the two methods generally produce comparable coherence despite the differing numerators in their corresponding equations (Eq. 9 and 14). However, we notice that the new PWC method produces consistently slightly higher coherence than the Mihanović et al. (2009) method. For example, their mean PWCs between y and y_2 at the scale of 8 after excluding the effect of y_4 are 1.00 and 0.97, respectively. This may indicate that the new method slightly outperforms the Mihanović et al. (2009) method because we expect that the coherence between y and y_2 at the scale (8) of y_2 is exactly 1.

Note that some unexpected high PWC can be produced in some domains by the new method. For example, at a scale of 32, PWC values between y and y_2 after excluding y_4 are not significant, but relatively high, partly because of small octaves (default of 1/12) per scale. This spurious unexpected high PWC is caused by low values in both the numerator (partly associated with the low coherence between response y and predictor variables y_2 at scale of 32) and denominator (partly associated with the high coherence between response y and excluding variable y_4 at a scale of 32) in Eq. (9). The same problem also exists in the Mihanović et al. (2009) method (Fig. 1b and 2b). Particularly, the Mihanović et al. (2009) method produces some positive infinite coherence (small black zones) between y (or z) and y_2 (or z_2) after eliminating the effect of y_2h_0 (or z_2h_0) (Fig. 2b) because of extremely low values in the both numerator and denominator term in Eq. (14). However, it seems that the

https://doi.org/10.5194/hess-2020-315
Preprint. Discussion started: 7 August 2020


Hydrology and Earth System Sciences
Discussions

307 domain with overestimation by the new method is very limited and it is located mainly
308 outside of the cones of influence. Anyway, the unexpected results can be easily ruled out
309 with knowledge of BWC between response and predictor variables.

310 Compared with the Mihanović et al. (2009) method, our new PWC method can be used
311 to deal with situations with more than one excluding variable, which is a knowledge gap.
312 Moreover, inclusion of phase information in the new PWC is another advantage of this
313 method.

314 **4.2 PWC with real data**

315 4.2.1 Free water evaporation

316 The PWC analysis indicates that the correlations between E and T after excluding the
317 effect of each of other three variables (RH, SH, and WS) were almost the same as those
318 indicated by the BWC (Fig. 4 and Fig. S3 of Sect. S5 in the Supplement). For example,
319 after excluding the effect of RH, E and T were positively correlated at the medium scales
320 (8–32 months). The PASC was 61% and mean PWC_{sig} value was 0.94, which was identical
321 to the case of BWC between E and T. The significant correlations at scales around 64
322 months between E and T from 1979 to 1992 were absent after eliminating the influence of
323 RH. This implies that the influence of mean temperature on *E* at these scales and years may
324 be associated with the negative influence of RH on both E and T (Fig. S3 of Sect. S5 in the
325 Supplement).

https://doi.org/10.5194/hess-2020-315
Preprint. Discussion started: 7 August 2020

Hydrology and Earth System Sciences
Discussions

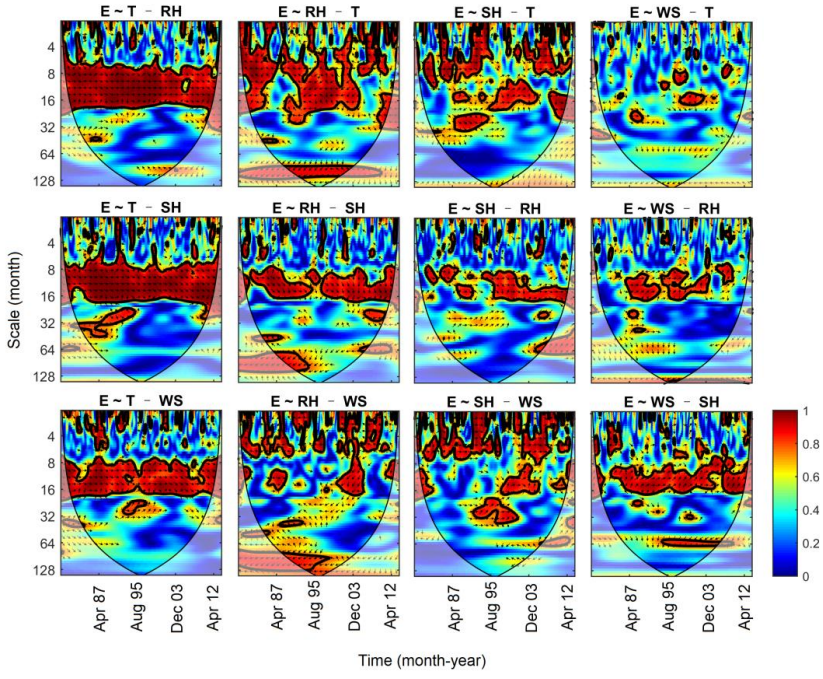

Figure 4.

Partial wavelet coherency (PWC) between evaporation (E) and each meteorological factor (T, mean temperature; RH, relative humidity; SH, sun hours; WS, wind speed) after excluding the effect of each of other three meteorological factors.

The PWC between E and RH depended on the excluding variable and scale (Fig. 4). The mean PWC and PASC between E and RH after excluding T were 0.60 and 34%, respectively, which are comparable to the mean BWC (0.62) and PASC (40%) between E and RH. The corresponding values after excluding SH and WS were 0.50 and 0.53 (PWC), 22% and 21% (PASC), respectively. In addition, compared with the BWC between E and RH, correlations between E and RH were almost absent at small scales (<8 months) and medium scales (8–32 months) after eliminating the influence of SH and WS, respectively. Therefore,

https://doi.org/10.5194/hess-2020-315
Preprint. Discussion started: 7 August 2020


Hydrology and Earth System Sciences
Discussions

338 excluding variable of T had less influence on the coherence between E and RH compared
339 with excluding variables of SH and WS. This is mainly because relative humidity and
340 temperature are correlated with E at different scales (Fig. S3 of Sect. S5 in the Supplement),
341 i.e., mean temperature affected E mainly at medium scales, while RH affected E across all
342 scales. However, the domain where SH and WS were correlated with E was subset of that
343 where RH and E were correlated (Fig. 4).

344 The relationships between E and sun hours after excluding other three factors were less
345 consistent. The areas with significant corrections were scattered over the whole frequency-
346 time domain but differed with excluding factors. The PASC varied from 12% (excluding
347 RH) to 20% (excluding T and WS), which is much lower than the PASC (28%) in the case
348 of BWC. The significant relationships between E and WS were only limited to very small
349 areas except for the case of SH being excluded, where E and wind speed were positively
350 correlated at scales of 8–16 months most of the time.

351 In general, the PASC decreased after excluding the effects of more factors (data not
352 shown). The correlations between E and each variable after eliminating the effects of all
353 other variables are shown in Fig. 5. The correlations between E and T were still significant
354 at the medium scales (8–32 months), where PASC value was 52% with mean PWC_{sig} of
355 0.92. The E was still correlated with RH at large scales (>32 months), where PASC value
356 was 35% with mean PWC_{sig} of 0.96. Interestingly, the domain with significant correlation
357 between E and SH and WS was very limited. This indicates that the influences of SH and
358 WS on E have already been covered by RH and T. This is in agreement with the MWC

https://doi.org/10.5194/hess-2020-315
Preprint. Discussion started: 7 August 2020

Hydrology and Earth System Sciences
Discussions

359 results that RH and T were the best to explain E variations at all scales. Although the RH
360 had the greatest mean wavelet coherence and PASC at the entire scale-location domains,
361 the PWC analysis seems to support that mean temperature was the most dominating factor
362 for free water evaporation at the 1-year cycle (8–16 months), which is the dominant scale
363 of E variation (Fig. S2 of Sect. S5 in the Supplement). This further verifies the suitability
364 of the Hargreaves model (only air temperature and incident solar radiation required)
365 (Hargreaves, 1989) for estimating potential evapotranspiration on the Chinese Loess
366 Plateau (Li, 2012).

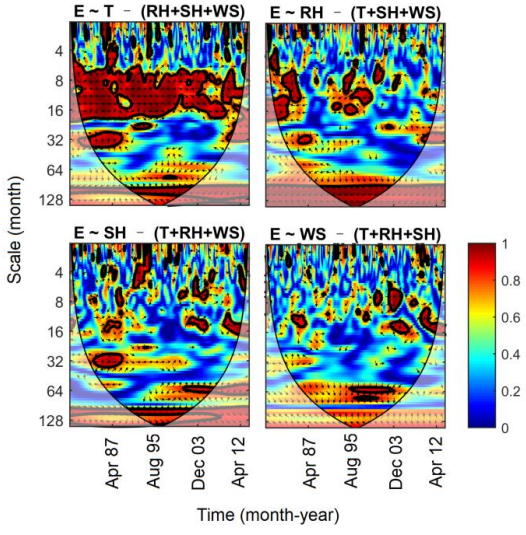

367

368 **Figure 5.**

369 Partial wavelet coherency (PWC) between evaporation (E) and each meteorological factor
370 (T, mean temperature; RH, relative humidity; SH, sun hours; WS, wind speed) after
371 excluding the effects of all other three factors.

https://doi.org/10.5194/hess-2020-315
Preprint. Discussion started: 7 August 2020


Hydrology and Earth System Sciences
Discussions

372 4.2.2 SWC

373 In spring, SWC at 0–0.2 m was significantly correlated with elevation, wetness index,
374 depth to $CaCO_3$ layer, and SOC at large scales (72–144 m); it was significantly correlated
375 with sand content, SOC, depth to $CaCO_3$ at medium scales (36–72 m) and bulk density at
376 scales of 36–144 m in the first half of the transect (Fig. S4 of Sect. S5 in the Supplement).
377 The PWC shows that SWC was not correlated with elevation after eliminating the effect of
378 SOC or depth to $CaCO_3$ (Fig. 6). By contrast, after the removal of the elevation's effect,
379 SWC was significantly correlated with SOC at scales of 36–144 m in the first half of the
380 transect and significantly correlated with depth to $CaCO_3$ layer at large scales (>100 m)
381 across the transect (Fig. 6). There were little correlations between SWC and wetness index
382 after eliminating the effect of elevation (Fig. 6). Therefore, the influences of elevation and
383 wetness index on SWC in spring might have been taken into account by SOC and depth to
384 $CaCO_3$ layer. Although elevation and wetness index are important drivers of snowmelt run-
385 off in spring (Hu et al., 2017), they did not contribute any more to explaining SWC
386 variations than SOC or depth to $CaCO_3$ layer did. The same holds for bulk density and sand
387 content whose influences on SWC were also limited after eliminating the effect of SOC
388 (Fig. 6). This was because SOC was negatively correlated with sand content at medium
389 scales (36–72 m) and bulk density at scales of 36–144 m in the first half of the transect (Fig.
390 S5 of Sect. S5 in the Supplement). Interestingly, the significant correlations between SWC
391 and SOC or depth to $CaCO_3$ layer still existed no matter what the excluding factors were.
392 For example, SWC was significantly correlated with depth to $CaCO_3$ layer at scales >130
393 m after the effect of SOC was removed; SWC was significantly correlated with SOC at

https://doi.org/10.5194/hess-2020-315
Preprint. Discussion started: 7 August 2020

Hydrology and Earth System Sciences
Discussions

large scales (>130 m) across the transect and at scales of 36–90 m at locations from 45 to 200 m after eliminating the effect of depth to $CaCO_3$ layer (Fig. 6). This further validates that the combination of depth to $CaCO_3$ layer and SOC were the best to explain SWC variations in spring (Hu et al., 2017).

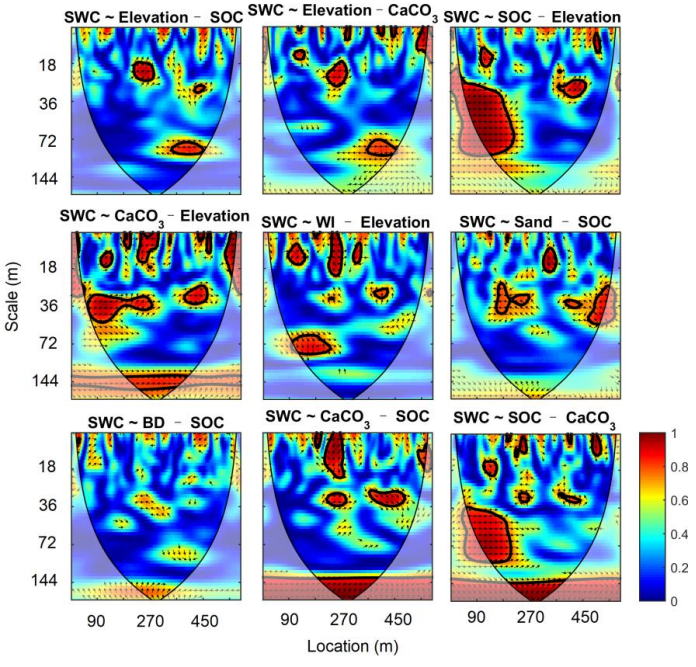

Figure 6.

Partial wavelet coherency (PWC) between soil water content (SWC) in spring and one environmental factor after excluding the effect of another environmental factor. SOC, soil organic carbon; $CaCO_3$, depth to the $CaCO_3$ layer; WI, wetness index; BD, bulk density.

In summer, SWC of 0–0.2 m tended to be significantly affected by aspect, slope, elevation, wetness index, clay, and sand at large scales (>90 m or 72–144 m) and by SOC, bulk density, and slope at medium scales (36–72 m) at locations from 45 to 450 m over the

https://doi.org/10.5194/hess-2020-315
Preprint. Discussion started: 7 August 2020


Hydrology and Earth System Sciences
Discussions

406 transect (Fig. S5 of Sect. S5 in the Supplement). The PWC analysis indicates that elevation,
407 wetness index, sand (not shown), clay, and BD had little influences on SWC after
408 eliminating the effect of slope in summer (Fig. 7). This is largely because slope was
409 significantly correlated to BD at medium scales and to elevation, wetness index, sand, and
410 clay at large scales (Fig. S6 of Sect. S5 in the Supplement). However, the influence of slope
411 on SWC was also limited after eliminating the effect of SOC (Fig. 7). By contrast, the effect
412 of SOC on SWC at the medium scales still existed at some locations after eliminating the
413 effects of slope and aspect (Fig. 7). This highlights the dominant role of SOC as a surrogate
414 of vegetation in driving evapo-transpiration loss at the slope (medium) scales (Hu et al.,
415 2017). As we expect, the effect of SOC on SWC at the medium scales disappeared after
416 eliminating the effect of BD because of the strong correlations between SOC and BD (Fig.
417 S5 of Sect. S5 in the Supplement). However, the effect of SOC on SWC was amplified at
418 large scales (>72 m) after excluding the effect of BD as also found in the artificial datasets
419 (Fig. 7). Interestingly, the significant correlation between SWC and aspect at large scales
420 (>90 m) persisted regardless the excluding variables (as an example, only PWC for
421 excluding variable of SOC is shown in Fig. 7). This highlights the dominant role of aspect
422 in driving soil water distribution at large scales in summer. Overall, the PWC analysis
423 further confirms that a combination of aspect and SOC was the best to explain SWC
424 variations in summer (Hu et al., 2017).

https://doi.org/10.5194/hess-2020-315
Preprint. Discussion started: 7 August 2020

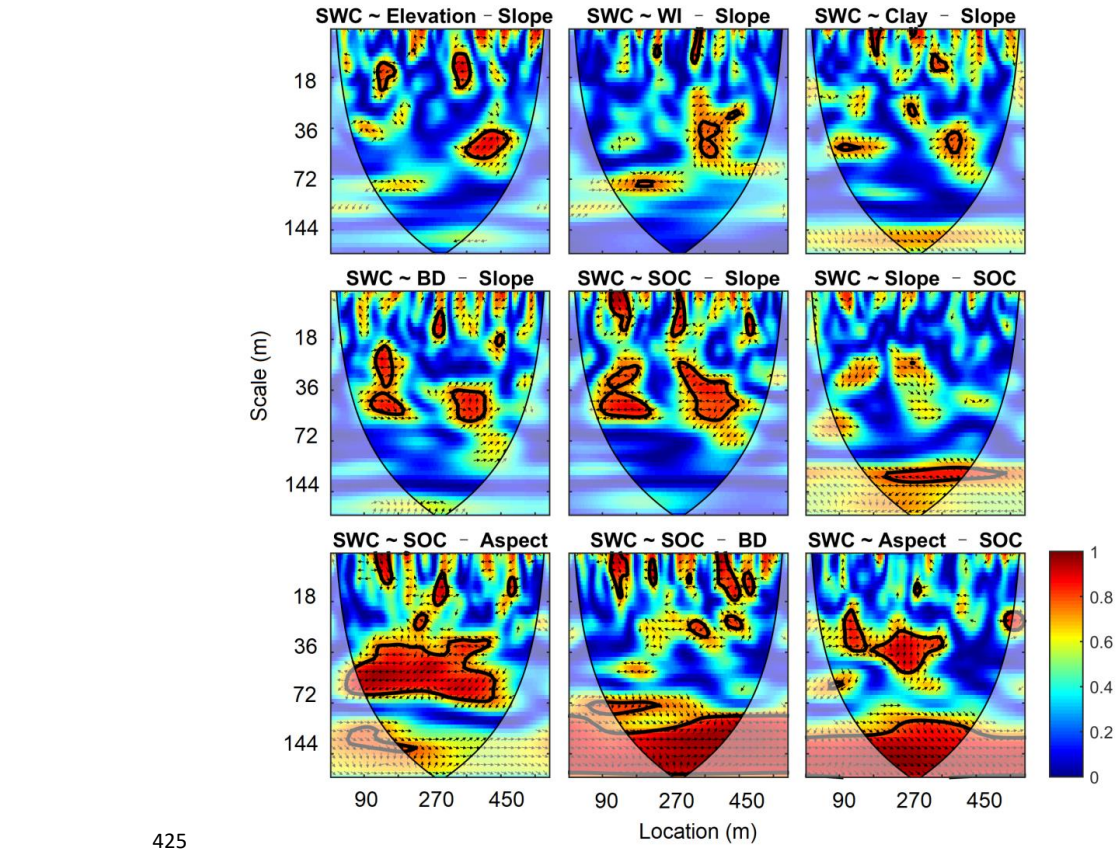

Figure 7.

Partial wavelet coherency (PWC) between soil water content (SWC) in summer and one environmental factor by excluding another environmental factor. SOC, soil organic carbon; Aspect, Cos(Aspect); WI, wetness index; BD, bulk density.

5. Conclusions

Partial wavelet coherency (PWC) is developed in this study to investigate scale-and location-specific bivariate relationships after excluding the effect of one or more variables in geosciences. This method was developed on the basis of partial coherence in the

https://doi.org/10.5194/hess-2020-315
Preprint. Discussion started: 7 August 2020


Hydrology and Earth System Sciences
Discussions

multivariate spectral case (Koopmans, 1995), and is an extension of previous work on PWC and WMC (Hu and Si, 2016; Mihanović et al., 2009). Compared with the previous PWC method (Mihanović et al., 2009), this new method produces slightly more accurate coherence. In addition, the new PWC method has the advantage of dealing with more than one excluding variable and providing the phase information associated with the PWC.

The new PWC method has been successfully tested with the artificial datasets. As we expect, regardless of the stationary and non-stationary case, there are no or reduced correlations between response and predictor variables in scale-location domains where the excluding variables are significantly correlated with the response variable. The new method also has the ability to deal with localized relationships. The new method was applied to two previously published datasets. The application has shown that the coherency between response and predictor variables was less affected by excluding other variables if the predictor variable had dominating roles in explaining the variations in the response variable. This application further confirmed the best combinations for explaining temporal variations in free water evaporation at the Changwu site in China and spatial variations in soil water content in the hummocky landscape in Saskatchewan, Canada.

Like the Mihanović et al. (2009) method (a previous PWC method), the new method has the risk to produce spurious correlations after excluding the effect from other variables. But this spurious high coherence can be easily identified with knowledge of BWC. So, caution should be taken to interpret those results. Similar to BWC and MWC, the new PWC also suffers from the multiple-testing problem (Schaefli et al., 2007; Schulte et al., 2015).

https://doi.org/10.5194/hess-2020-315
Preprint. Discussion started: 7 August 2020


Hydrology and Earth System Sciences
Discussions

455 Therefore, the new method can benefit from a better statistical significance testing method.

456 Our artificial datasets and two real-world datasets have verified that our PWC method
457 provides an effective tool to untangle the bivariate relationships at multiple scale-location
458 domains after eliminating the effects of other variables. The new method provides a much
459 needed data-driven tool for unraveling underlining mechanisms in a spatial or temporal
460 series. Thus, combining with wavelet transform, BWC, and MWC, the new PWC method
461 can be used to detect various processes in geosciences, such as stream flow, droughts,
462 greenhouse gas emissions (e.g., N_2O, CO_2, and CH_4), atmospheric circulation, and oceanic
463 processes (e.g., EI Niño-Southern Oscillation).

464 **Acknowledgements**

465 The Matlab codes for calculating partial wavelet coherency are available in the Supplement
466 (Sect. S1–S3). The codes are developed based on those provided by Aslak Grinsted
467 (http://www.glaciology.net/wavelet-coherence) and Wei Hu and Bing Si
468 (https://www.hydrol-earth-syst-sci.net/20/3183/2016/hess-20-3183-2016-supplement.pdf).
469 The preparation of this manuscript was partly supported by The New Zealand Institute for
470 Plant and Food Research Limited under the *Sustainable Agro-ecosystems* programme.

471 **References**

472 Aloui, C., Hkiri, B., Hammoudeh, S., and Shahbaz, M.: A multiple and partial wavelet
473 analysis of the oil price, inflation, exchange rate, and economic growth nexus in Saudi
474 Arabia, Emerging Markets Finance and Trade, 54, 935-956, 2018.

https://doi.org/10.5194/hess-2020-315
Preprint. Discussion started: 7 August 2020

475 Altarturi, B. H., Alshammari, A. A., Saiti, B., and Erol, T.: A three-way analysis of the
476 relationship between the USD value and the prices of oil and gold: A wavelet analysis,
477 AIMS Energy, 6, 487, 2018.
478 Biswas, A., Chau, H. W., Bedard-Haughn, A. K., and Si, B. C.: Factors controlling soil
479 water storage in the hummocky landscape of the Prairie Pothole Region of North America,
480 Can J Soil Sci, 92, 649-663, 2012.
481 Biswas, A. and Si, B. C.: Identifying scale specific controls of soil water storage in a
482 hummocky landscape using wavelet coherency, Geoderma, 165, 50-59, 2011a.
483 Biswas, A. and Si, B. C.: Revealing the controls of soil water storage at different scales in
484 a hummocky landscape, Soil Sci Soc Am J, 75, 1295-1306, 2011b.
485 Centeno, L. N., Hu, W., Timm, L. C., She, D. L., Ferreira, A. D., Barros, W. S., Beskow, S.,
486 and Caldeira, T. L.: Dominant Control of Macroporosity on Saturated Soil Hydraulic
487 Conductivity at Multiple Scales and Locations Revealed by Wavelet Analyses, Journal of
488 Soil Science and Plant Nutrition, 20, 2020.
489 Das, N. N. and Mohanty, B. P.: Temporal dynamics of PSR-based soil moisture across
490 spatial scales in an agricultural landscape during SMEX02: A wavelet approach, Remote
491 Sensing of Environment, 112, 522-534, 2008.
492 Graf, A., Bogena, H. R., Drüe, C., Hardelauf, H., Pütz, T., Heinemann, G., and Vereecken,
493 H.: Spatiotemporal relations between water budget components and soil water content in a
494 forested tributary catchment, Water Resour Res, 50, 4837-4857, 2014.
495 Grinsted, A., Moore, J. C., and Jevrejeva, S.: Application of the cross wavelet transform
496 and wavelet coherence to geophysical time series, Nonlinear Processes in Geophysics, 11,

https://doi.org/10.5194/hess-2020-315
Preprint. Discussion started: 7 August 2020

561-566, 2004.

Gu, X. F., Sun, H. G., Tick, G. R., Lu, Y. H., Zhang, Y. K., Zhang, Y., and Schilling, K.: Identification and Scaling Behavior Assessment of the Dominant Hydrological Factors of Nitrate Concentrations in Streamflow, J Hydrol Eng, 25, 06020002, 2020.

Hargreaves, G. H.: Accuracy of estimated reference crop evapotranspiration, Journal of irrigation and drainage engineering, 115, 1000-1007, 1989.

Hu, W. and Si, B. C.: Technical note: Multiple wavelet coherence for untangling scale-specific and localized multivariate relationships in geosciences, Hydrol Earth Syst Sc, 20, 3183-3191, 2016.

Hu, W., Si, B. C., Biswas, A., and Chau, H. W.: Temporally stable patterns but seasonal dependent controls of soil water content: Evidence from wavelet analyses, Hydrol Process, 31, 3697-3707, 2017.

Jia, X., Zha, T., Gong, J., Zhang, Y., Wu, B., Qin, S., and Peltola, H.: Multi-scale dynamics and environmental controls on net ecosystem CO_2 exchange over a temperate semiarid shrubland, Agricultural and Forest Meteorology, 259, 250-259, 2018.

Kenney, J. F. and Keeping, E. S.: Mayhematics of Statistics, D. van Nostrand, 1939.

Koopmans, L. H.: The spectral analysis of time series, Elsevier, 1995.

Lakshmi, V., Piechota, T., Narayan, U., and Tang, C.: Soil moisture as an indicator of weather extremes, Geophysical research letters, 31, L11401, 2004.

Li, H., Dai, S., Ouyang, Z., Xie, X., Guo, H., Gu, C., Xiao, X., Ge, Z., Peng, C., and Zhao, B.: Multi-scale temporal variation of methane flux and its controls in a subtropical tidal salt marsh in eastern China, Biogeochemistry, 137, 163-179, 2018.

https://doi.org/10.5194/hess-2020-315
Preprint. Discussion started: 7 August 2020

519 Li, Z.: Applicability of simple estimating method for reference crop evapotranspiration in
520 Loess Plateau, Transactions of the Chinese Society of Agricultural Engineering, 28, 106-
521 111, 2012.
522 Mares, I., Mares, C., Dobrica, V., and Demetrescu, C.: Comparative study of statistical
523 methods to identify a predictor for discharge at Orsova in the Lower Danube Basin,
524 Hydrological Sciences Journal, 65, 371-386, 2020.
525 Mihanović, H., Orlić, M., and Pasarić, Z.: Diurnal thermocline oscillations driven by tidal
526 flow around an island in the Middle Adriatic, Journal of Marine Systems, 78, S157-S168,
527 2009.
528 Mutascu, M. and Sokic, A.: Trade openness-CO_2 emissions nexus: a wavelet evidence from
529 EU, Environmental Modeling & Assessment, 25, 1-18, 2020.
530 Nalley, D., Adamowski, J., Biswas, A., Gharabaghi, B., and Hu, W.: A multiscale and
531 multivariate analysis of precipitation and streamflow variability in relation to ENSO, NAO
532 and PDO, J Hydrol, 574, 288-307, 2019.
533 Ng, E. K. and Chan, J. C.: Geophysical applications of partial wavelet coherence and
534 multiple wavelet coherence, Journal of Atmospheric and Oceanic Technology, 29, 1845-
535 1853, 2012a.
536 Ng, E. K. and Chan, J. C.: Interannual variations of tropical cyclone activity over the north
537 Indian Ocean, International Journal of Climatology, 32, 819-830, 2012b.
538 Polansky, L., Wittemyer, G., Cross, P. C., Tambling, C. J., and Getz, W. M.: From moonlight
539 to movement and synchronized randomness: Fourier and wavelet analyses of animal
540 location time series data, Ecology, 91, 1506-1518, 2010.

https://doi.org/10.5194/hess-2020-315
Preprint. Discussion started: 7 August 2020

Rathinasamy, M., Agarwal, A., Parmar, V., Khosa, R., and Bairwa, A.: Partial wavelet coherence analysis for understanding the standalone relationship between Indian Precipitation and Teleconnection patterns, arXiv preprint arXiv:1702.06568, 2017. 2017.

Schaefli, B., Maraun, D., and Holschneider, M.: What drives high flow events in the Swiss Alps? Recent developments in wavelet spectral analysis and their application to hydrology, Adv Water Resour, 30, 2511-2525, 2007.

Schulte, J., Duffy, C., and Najjar, R.: Geometric and topological approaches to significance testing in wavelet analysis, Nonlinear Processes in Geophysics, 22, 2015.

Sen, A., Chaudhury, P., and Dutta, K.: On the co-movement of crude, gold prices and stock index in Indian market, arXiv preprint arXiv:1904.05317, 2019. 2019.

Si, B. C.: Spatial scaling analyses of soil physical properties: A review of spectral and wavelet methods, Vadose Zone Journal, 7, 547-562, 2008.

Si, B. C. and Zeleke, T. B.: Wavelet coherency analysis to relate saturated hydraulic properties to soil physical properties, Water Resour Res, 41, W11424, 2005.

Song, X. M., Zhang, C. H., Zhang, J. Y., Zou, X. J., Mo, Y. C., and Tian, Y. M.: Potential linkages of precipitation extremes in Beijing-Tianjin-Hebei region, China, with large-scale climate patterns using wavelet-based approaches, Theoretical and Applied Climatology, 141, 1251-1269, 2020.

Su, L., Miao, C., Duan, Q., Lei, X., and Li, H.: Multiple‐wavelet coherence of world's large rivers with meteorological factors and ocean signals, Journal of Geophysical Research: Atmospheres, 124, 4932-4954, 2019.

Tan, X., Gan, T. Y., and Shao, D.: Wavelet analysis of precipitation extremes over Canadian

https://doi.org/10.5194/hess-2020-315
Preprint. Discussion started: 7 August 2020


Hydrology and Earth System Sciences
Discussions

563 ecoregions and teleconnections to large - scale climate anomalies, Journal of Geophysical
564 Research: Atmospheres, 121, 14469-14486, 2016.
565 Torrence, C. and Compo, G. P.: A practical guide to wavelet analysis, Bulletin of the
566 American Meteorological society, 79, 61-78, 1998.
567 Wu, K., Zhu, J., Xu, M., and Yang, L.: Can crude oil drive the co-movement in the
568 international stock market? Evidence from partial wavelet coherence analysis, The North
569 American Journal of Economics and Finance, 2020. 101194, 2020.
570 Yan, R. and Gao, R. X.: A tour of the tour of the Hilbert-Huang transform: an empirical tool
571 for signal analysis, IEEE Instrumentation & Measurement Magazine, 10, 40-45, 2007.
572 Zhao, R., Biswas, A., Zhou, Y., Zhou, Y., Shi, Z., and Li, H.: Identifying localized and scale-
573 specific multivariate controls of soil organic matter variations using multiple wavelet
574 coherence, Sci Total Environ, 643, 548-558, 2018.